

## Questioning the adequacy of certain quantum arrival-time distributions

Siddhant Das \**Mathematisches Institut, Ludwig-Maximilians-Universität München, Theresienstraße 39, 80333 München, Germany*Ward Struyve †*Instituut voor Theoretische Fysica, KU Leuven, Celestijnenlaan 200D, 3001 Leuven, Belgium  
and Centrum voor Logica en Filosofie van de Wetenschappen, KU Leuven, Kardinaal Mercierplein 2, 3000 Leuven, Belgium*

(Received 31 May 2021; accepted 13 September 2021; published 18 October 2021)

It is shown that a class of exponentially decaying time-of-arrival probability distributions, suggested by Włodarz [Phys. Rev. A **65**, 044103 (2002)], Marchewka and Schuss [Phys. Lett. A **240**, 177 (1998), Phys. Rev. A **63**, 032108 (2001); **65**, 042112 (2002)], and Jurman and Nikolić [Phys. Lett. A **396**, 127247 (2021)], and a semiclassical distribution implicit in time-of-flight momentum measurements do not show the expected behavior for a Gaussian wave train. This casts doubts on the physical adequacy of these arrival-time proposals. In contrast, the quantum flux distribution (a special case of the Bohmian arrival-time distribution) displays the expected behavior.

DOI: [10.1103/PhysRevA.104.042214](https://doi.org/10.1103/PhysRevA.104.042214)

### I. INTRODUCTION

In view of the experimentally driven genesis of quantum mechanics and its notable empirical successes, it is a great surprise that a straightforward question such as *how long* it takes for a quantum particle to strike the detector surface in a double-slit experiment could be even more problematic than the question of *where*, in such an experiment, the particle strikes the detector surface. While the second question pertaining to the ubiquitous interference pattern is discussed in every quantum mechanics textbook and is experimentally well-established, the former concerning the arrival (or detection) time of the particle amenable to laboratory time-of-flight (TOF) experiments [1] is a matter of an ongoing debate.

This seems almost paradoxical given that TOF measurements are the quintessence of methods determining, e.g., energies and momenta of particles [2–5], chemical reaction dynamics (as in the Rydberg tagging TOF technique [6,7]), or the temperature of single trapped atoms or ions [8,9]. However, it is not quantum mechanics that is invoked to interpret the TOF measurements in these cases. Instead, one employs various *Ansätze* and heuristics based on either Newtonian mechanics or geometric optics, whose capabilities for describing the data are highly questionable (especially in single-particle experiments featuring wave-packet coherence).

Nevertheless, over the past decades, an increasing number of physicists have endeavored to formulate a first-principles description of arrival times within quantum mechanics, resulting in a multitude of disparate theoretical proposals for

computing the arrival-time distribution<sup>1</sup>  $\Pi(\tau)$  of a quantum particle [10–12]. However, experiments designed to help choose between competing viewpoints have been slow in coming.

The TOF distributions suggested in the literature can be divided into two broad categories. First, ideal (or intrinsic) arrival-time distributions that are *apparatus-independent* theoretical predictions, given by some functional of the initial wave function  $\psi(x, 0)$  and the geometrical surface of the detector (typically a single point on a line in one-dimensional discussions). A notable example is the quantum flux distribution

$$\Pi_{\text{QF}}(\tau) = \frac{\hbar}{m} \text{Im}[\psi^*(L, \tau) \partial_x \psi(L, \tau)], \quad (1)$$

applicable for a particle of mass  $m$  arriving at the point  $x = L$  on a line. Here  $\psi(x, t)$  denotes its wave function at time  $t$ , a solution of Schrödinger's equation

$$i\hbar \frac{\partial \psi(x, t)}{\partial t} = -\frac{\hbar^2}{2m} \frac{\partial^2 \psi(x, t)}{\partial x^2} + V(x, t) \psi(x, t), \quad (2)$$

with initial condition  $\psi(x, 0)$ . The quantum flux distribution has been arrived at from various theoretical viewpoints, in particular, as the arrival-time distribution in Bohmian mechanics (de Broglie–Bohm or pilot-wave theory) [13–15] in the absence of backflow (see [16], p. 6).<sup>2</sup> Another well-known

<sup>1</sup> $\Pi(\tau)d\tau$  is the probability that a particle prepared in a state  $\psi(x, 0)$  at time zero is registered on a specified detector between time  $\tau$  and  $\tau + d\tau$ .

<sup>2</sup>Indeed, there are examples where quantum backflow occurs [17–21] for which (1) fails to be a meaningful arrival-time distribution. This defect is remedied by the Bohmian arrival-time distribution, which is well-defined for all wave functions.

\*Siddhant.Das@physik.uni-muenchen.de

†ward.struyve@kuleuven.be

TABLE I. Exponentially decaying arrival-time proposals and their intensity functions (the wave functions  $\tilde{\psi}$  and  $\psi_c$  are defined in Sec. III).

Proponents	$\lambda(t)$	Ref.
Włodarz	$\lambda_0  \psi(L, t) ^2$	[39]
Marchewka and Schuss	$(\lambda' \epsilon / \pi)  \partial_x \tilde{\psi}(L, t) ^2$	[36]
Jurman and Nikolić	$\frac{1}{\delta t} \int_L^{L+\Delta L} dx  \psi_c(x, t) ^2$	[33]

example applicable for freely moving particles,  $V(x, t) = 0$ , is the Aharonov-Bohm (see [22], Sec. 3) and Kijowski [23] arrival-time distribution (see [16], Sec. 2), which is typically indistinguishable from  $\Pi_{\text{QF}}(\tau)$  in the far-field or scattering regime accessible to present-day experiments.

Yet another ideal arrival-time distribution often implicit in TOF momentum measurements is the semiclassical distribution

$$\Pi_{\text{SC}}(\tau) = \frac{mL}{\hbar\tau^2} \left| \tilde{\psi} \left( \frac{mL}{\hbar\tau} \right) \right|^2, \quad (3)$$

where

$$\tilde{\psi}(k) = \frac{1}{\sqrt{2\pi}} \int_{-\infty}^{\infty} dx \psi(x, 0) e^{-ikx} \quad (4)$$

is the Fourier transform of the wave function prepared at *time zero* [4,5,24,25]. This distribution is typically motivated along the following lines: For a classical trajectory  $x(t) = x(0) + pt/m$ , with  $x(0) \ll L$ , the arrival time of the particle is approximately given by  $\tau = mL/p$ . The above distribution  $\Pi_{\text{SC}}(\tau)$  is then obtained by considering this classical arrival-time formula, assuming that the width of  $\psi(x, 0)$  is much smaller than  $L$  and that the momentum  $p$  is distributed according to the quantum mechanical momentum distribution  $\hbar^{-1} |\tilde{\psi}(p/\hbar)|^2$  (see [26], p. 21). For a suitably localized  $\psi(x, 0)$ , the semiclassical distribution (3) is also recovered from  $\Pi_{\text{QF}}(\tau)$  for large  $L$  and large  $\tau$  [13].

The second category is that of nonideal or measurement-inspired TOF distributions that involve a model of the detector. Various suggestions have been put forward, e.g., simple absorbing boundary conditions [27,28], complex potentials [29–31], wave-function collapse (both detector induced [32,33] and spontaneous [34,35]), path integrals with absorbing boundaries [36], a variety of quantum clocks (see [12], Chap. 8), and even a timeless formulation of quantum measurement [37]. An overview of these proposals, including an experimental setup for distinguishing one from another [and in particular from  $\Pi_{\text{QF}}(\tau)$ ], will appear in [38].

In what follows, we focus on a class of nonideal TOF distributions [33,36,39] that have the form

$$\Pi(\tau) = \lambda(\tau) \exp \left( - \int_0^\tau dt \lambda(t) \right), \quad (5)$$

where  $\lambda(t)$  is the so-called intensity function for which various proposals exist (see Table I). This distribution is normalized as

$$\int_0^\infty d\tau \Pi(\tau) + P(\infty) = 1, \quad (6)$$

where

$$P(\infty) = \lim_{\tau \rightarrow \infty} \frac{\Pi(\tau)}{\lambda(\tau)} \quad (7)$$

is a nondetection probability, accounting for the fraction of experimental runs in which the particle never arrives at  $L$ . To derive (5) a time interval  $[0, \tau]$  is considered (see [39], p. 2), discretized into small time steps  $\Delta t = \tau/N$ , where  $\lambda(t_n)\Delta t$  is the probability for the particle to be detected between time  $t_n = n\Delta t$  and  $t_{n+1} = (n+1)\Delta t$ ,  $n = 0, 1, 2, \dots, N-1$ . Further, assuming *independent* probabilities at each time step,<sup>3</sup> the probability for the particle to be detected between time  $t_{N-1}$  and  $t_N (= \tau)$  is simply

$$\lambda(t_{N-1})\Delta t \prod_{n=0}^{N-2} [1 - \lambda(t_n)\Delta t]. \quad (8)$$

By taking the limit  $\Delta t \rightarrow 0$ , or equivalently  $N \rightarrow \infty$ , of (8), the time-of-arrival density (5) is obtained. The intensity function  $\lambda$  is supposed to follow from the physics of the detector.

We will challenge these proposals by considering a train of Gaussian wave packets that initially have the same width and are moving with the same velocity towards the detector. By choosing the parameters so that each Gaussian wave packet reaches the detector one by one without significant spreading, it is expected on the basis of quasiclassical reasoning that each packet will contribute in the same way to the arrival-time distribution. In particular, it is anticipated that the arrival-time distribution will display peaks of identical shape and height at times roughly corresponding to the hitting times of individual packets. However, we will show that this is not the case for the proposals listed in Table I. While these distributions display peaks at the expected wave-packet arrival times, the peaks are exponentially damped.

The outline of the paper is as follows. In Sec. II the Gaussian train is introduced. The analysis of the exponential proposals for this wave function follows in Sec. III. The semiclassical distribution is treated in Sec. IV. We summarize and discuss our results in Sec. V.

## II. GAUSSIAN WAVE TRAIN

We direct our attention to the dynamics on a line, the detector occupying the interval  $(L, L + \Delta L)$ . Consider first a single Gaussian wave packet, initially ( $t = 0$ ) centered at  $x = 0$ , to the left of the detector, given by

$$\phi(x, 0) = \frac{1}{\sqrt{\sigma} \sqrt{\pi}} \exp \left( -\frac{x^2}{2\sigma^2} + \frac{i}{\epsilon} vx \right). \quad (9)$$

Here  $\epsilon = \hbar/m$ ,

$$\sigma \ll L \quad (10)$$

is the width of the wave packet, and  $v > 0$  is the phase velocity. Under the free Schrödinger evolution, with the

<sup>3</sup>This generates an inhomogeneous Poisson point process with rate  $\lambda(t)$ .

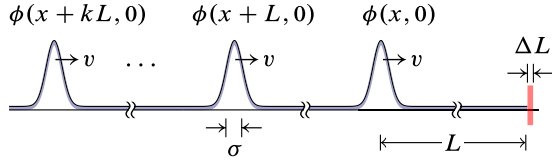


FIG. 1. Train of Gaussian wave packets moving towards the detector.

Hamiltonian

$$H = -\frac{\hbar^2}{2m} \frac{d^2}{dx^2}, \tag{11}$$

the time-dependent packet is

$$\begin{aligned} \phi(x, t) &= e^{-itH/\hbar} \phi(x, 0) \\ &= \frac{1}{\sqrt{\sigma(t)}\sqrt{\pi}} \exp \left\{ -\frac{\sigma}{\sigma(t)} \left[ \frac{x^2}{2\sigma^2} - \frac{iv}{\epsilon} \left( x - \frac{vt}{2} \right) \right] \right\}, \end{aligned} \tag{12}$$

where

$$\sigma(t) = \sigma \left( 1 + i \frac{\epsilon t}{\sigma^2} \right). \tag{13}$$

The amplitude of this packet is

$$|\phi(x, t)| = \frac{1}{\sqrt{|\sigma(t)|}\sqrt{\pi}} \exp \left( -\frac{1}{2} \frac{(x - vt)^2}{|\sigma(t)|^2} \right). \tag{14}$$

It follows that the center of the packet arrives at the detector at time

$$\tau_0 = \frac{L}{v}; \tag{15}$$

hence the corresponding time-of-arrival distribution, denoted by  $\Pi_0(\tau - \tau_0)$ , is expected to be peaked around  $\tau_0$ .

We will assume that the packet suffers negligible distortion during  $0 < t < \tau_0$ . This is guaranteed if

$$\frac{\epsilon \tau_0}{\sigma^2} = \frac{\epsilon L}{\sigma^2 v} \ll 1, \tag{16}$$

which will be referred to as the *no-spreading condition*. In this case,

$$|\phi(x, t)| \approx |\phi(x - vt, 0)| \tag{17}$$

for  $0 < t < \tau_0$ .

Consider now an initial superposition of  $N$  Gaussian wave packets with the same width and velocity, but centered at  $x = -kL, k = 0, 1, \dots, N - 1$ ,

$$\psi(x, 0) = \frac{1}{\sqrt{N}} \sum_{k=0}^{N-1} \phi(x + kL, 0), \tag{18}$$

depicted in Fig. 1. It evolves into

$$\psi(x, t) = e^{-itH/\hbar} \psi(x, 0) = \frac{1}{\sqrt{N}} \sum_{k=0}^{N-1} \phi(x + kL, t), \tag{19}$$

where  $\phi(\cdot, t)$  is given by (12). Assuming

$$N\tau_0 \ll \sigma^2/\epsilon, \tag{20}$$

the wave packets will remain nonoverlapping until time  $N\tau_0$ , the time at which the  $N$ th wave packet of the Gaussian train strikes  $x = L$ . As a consequence,

$$\begin{aligned} |\psi(x, t)|^2 &\approx \frac{1}{N} \sum_{k=0}^{N-1} |\phi(x + kL, t)|^2 \\ &\stackrel{(17)}{\approx} \frac{1}{N} \sum_{k=0}^{N-1} |\phi(x + kL - vt, 0)|^2 \end{aligned} \tag{21}$$

for all  $0 < t < N\tau_0$ .

In this event, one expects the arrival-time distribution to have  $N$  peaks of nearly identical shape and height centered at times  $k\tau_0, k = 1, 2, \dots, N$ , i.e.,

$$\Pi(\tau) \approx \frac{1}{N} \sum_{k=1}^N \Pi_0(\tau - k\tau_0). \tag{22}$$

That is, the Gaussian wave packets in the train arrive at the detector one by one with time delays of  $\tau_0$ , so there should be a peak in the arrival-time density, which has the same shape for any Gaussian wave packet.

The quantum flux TOF distribution (1), i.e.,

$$\Pi_{\text{QF}}(\tau) \approx \frac{v}{N\sqrt{\pi}\sigma} \sum_{k=1}^N \exp \left( -\frac{v^2}{\sigma^2} (\tau - k\tau_0)^2 \right), \tag{23}$$

which happens to agree with the Bohmian distribution in this case (due to the absence of backflow) is of the expected form (22). Note that the integral of (23) over all  $\tau > 0$  is approximately unity; hence it predicts a zero nondetection probability as per Eq. (6).

### III. EXPONENTIAL DISTRIBUTIONS

The arrival-time distributions proposed in [33,36,39] do not have the form (22) for the Gaussian wave train. Instead, the probability density is exponentially falling off. In particular, assuming only (10) and (20), we will show that the intensity functions (Table I) take, for the Gaussian wave train (18), the form

$$\lambda(t) \approx \frac{1}{N} \sum_{k=1}^N \lambda_0(t - k\tau_0), \tag{24}$$

where  $\lambda_0(t)$  is the intensity function corresponding to  $\phi(x, t)$  supported on  $|t - \tau_0| \leq \Delta\tau$ , with  $2\Delta\tau$  the duration over which  $\phi$  sweeps over the detector, approximately equal to  $3\sigma/v$ . This implies that the TOF distribution  $\Pi(\tau)$  decays exponentially over time owing to the exponential factor in (5). In fact, for  $k\tau_0 < \tau < (k + 1)\tau_0$ , we have

$$\exp \left( -\int_0^\tau dt \lambda(t) \right) \approx \exp \left( -k \int_{\tau_0 - \Delta\tau}^{\tau_0 + \Delta\tau} dt \lambda_0(t) \right). \tag{25}$$

It follows that the expected behavior (22) cannot hold.

### A. Włodarz proposal

Using (21), we readily obtain the intensity function  $\lambda_W$  given in Table I,

$$\lambda_W(t) \approx \frac{\lambda_0}{N} \sum_{k=1}^N |\phi(kL - vt, 0)|^2, \quad (26)$$

which implies the property (24).

### B. Marchewka-Schuss proposal

To calculate  $\lambda_{MS}(t)$  (cf. Table I) we need  $\bar{\psi}(x, t)$ , which is the solution of Schrödinger's equation on the half-line  $(-\infty, L]$  with the initial condition  $\psi(x, 0)$  and Dirichlet boundary condition at  $x = L$ . It is given by

$$\bar{\psi}(x, t) = \theta(x - L)[\psi(x, t) - \psi(2L - x, t)], \quad (27)$$

where  $\theta$  is Heaviside's step function.<sup>4</sup> (This state is only approximately normalized to unity as (18) has support on  $[L, \infty)$ ). The (left) derivative at  $L$  is  $\partial_x \bar{\psi}(L, t) = 2\partial_x \psi(L, t)$  and

$$|\partial_x \bar{\psi}(L, t)|^2 \approx \frac{4}{N} \sum_{k=1}^N |\partial_x \phi(kL, t)|^2, \quad (28)$$

noting that  $\phi(kL, t)$  and hence  $\partial_x \phi(kL, t)$  for different  $k$  are approximately nonoverlapping due to (20).

To evaluate the summands we use (12), obtaining

$$|\partial_x \phi(x, t)|^2 = \left| \frac{\phi(x, t)}{\sigma(t)} \right|^2 \left[ \left( \frac{x}{\sigma} \right)^2 + \left( \frac{v\sigma}{\epsilon} \right)^2 \right], \quad (29)$$

which is exact, but in view of (20),

$$|\partial_x \phi(kL, t)|^2 \approx \left( \frac{v}{\epsilon} \right)^2 |\phi(kL, t)|^2 \quad (30)$$

for  $k = 1, 2, \dots, N$  and  $0 < t < N\tau_0$ . Then, using (17) and (28), we arrive at

$$\lambda_{MS}(t) \approx \frac{4v^2 \lambda'}{N\pi\epsilon} \sum_{k=1}^N |\phi(kL - vt, 0)|^2. \quad (31)$$

In this case, the intensity function approximately agrees with  $\lambda_W$  [Eq. (26)] (up to a proportionality factor). Again the property (24) is obtained.

### C. Jurman-Nikolić proposal

To calculate  $\lambda_{JN}(t)$ , given in Table I, we need  $\psi_c(x, t)$ , defined by

$$\psi_c(x, t) = e^{-i\delta t H/\hbar} e^{-i(t-\delta t)\bar{H}/\hbar} \psi(x, 0), \quad (32)$$

where  $H$  is the free Hamiltonian (11) and

$$\bar{H} = \begin{cases} 0 & \text{for } L < x < L + \Delta L \\ H & \text{otherwise.} \end{cases}$$

It is convenient to rewrite (32) as

$$\psi_c(x, t) = e^{-i\delta t H/\hbar} \eta(x, t - \delta t), \quad (33)$$

where  $\eta(x, t)$  solves Schrödinger's equation with the Hamiltonian  $\bar{H}$  and initial condition  $\psi(x, 0)$ .

Since  $\bar{H}$  is defined piecewise, we have  $\partial_t \eta = 0$  in the detector region, and consequently

$$\eta(x, t) = \psi(x, 0) \quad \text{for } L < x < L + \Delta L, \quad (34)$$

at any given time. For  $x < L$  and  $x > L + \Delta L$ ,  $i\partial_t \eta = -\epsilon \partial_x^2 \eta$  holds with boundary conditions  $\eta(x, t) \rightarrow 0$  as  $x \rightarrow \pm\infty$  [dictated by the specified initial condition  $\psi(x, 0)$ ]. In addition to this, we need suitable boundary or interface conditions at  $x = L$  and  $L + \Delta L$  to obtain a *unique* solution for  $\eta$ , which were not specified in [33]. A natural choice is to make  $\eta$  continuous at these points, i.e.,  $\eta(L^-, t) = \eta(L^+, t)$ , and likewise at  $L + \Delta L$ .<sup>5</sup> Given that  $\psi(x, 0)$  is supported on  $(-\infty, L]$  [see [33], Eq. (15)], it follows that  $\eta(x, 0) = 0$  for  $x > L$  at all times. In particular,  $\eta(x, t) = \bar{\psi}(x, t)$  [Eq. (27)], the solution of Schrödinger's equation with Dirichlet boundary conditions at  $x = L$ .

Our initial wave function (18) is actually nonzero in the region  $[L, \infty)$  but, as before, we will ignore its tail beyond  $x = L$ , given (10). In any case, Eq. (33) reduces to

$$\psi_c(x, t) = e^{-i\delta t H/\hbar} \bar{\psi}(x, t - \delta t). \quad (35)$$

To evaluate this for the Gaussian train, consider, for  $0 \leq k < N$ , the function  $\phi_c$  defined by

$$\begin{aligned} \phi_c(x + kL, t) &:= e^{-i\delta t H/\hbar} e^{-i(t-\delta t)\bar{H}/\hbar} \phi(x + kL, 0) \\ &= e^{-i\delta t H/\hbar} e^{-i(t-k\tau_0-\delta t)\bar{H}/\hbar} \\ &\quad \times e^{-ik\tau_0 \bar{H}/\hbar} \phi(x + kL, 0) \\ &= e^{-i\delta t H/\hbar} e^{-i(t-k\tau_0-\delta t)\bar{H}/\hbar} \bar{\phi}(x + kL, k\tau_0). \end{aligned} \quad (36)$$

Since  $\phi(x + kL, k\tau_0)$  is centered at  $x = 0$  and has a width  $|\sigma(k\tau_0)| \approx \sigma$  in view of the no-spreading condition (20) [cf. Eq. (13)], we have

$$\bar{\phi}(x + kL, k\tau_0) \approx \phi(x + kL, k\tau_0).$$

Using (17) and (20), the amplitude of this wave function satisfies

$$|\phi(x + kL, k\tau_0)| \approx |\phi(x, 0)|. \quad (38)$$

Its phase is

$$\begin{aligned} \arg[\phi(x + kL, k\tau_0)] &= \arg[\phi(x, 0)] - \frac{\epsilon k\tau_0}{2\sigma^2} \\ &\quad + \frac{k\tau_0}{2} \left( \frac{v^2}{\epsilon} + \epsilon \frac{(x/\sigma)^2}{|\sigma(k\tau_0)|^2} \right). \end{aligned} \quad (39)$$

Equation (20), together with the condition  $|x| \lesssim 3\sigma$  valid within the bulk of the support of the wave function, allows us to neglect both the second term and the second term in large parentheses; thus

$$\arg[\phi(x + kL, k\tau_0)] \approx \arg[\phi(x, 0)] + k \frac{vL}{2\epsilon}.$$

<sup>4</sup>The wave function  $\bar{\psi}$  is defined to be zero for  $x > L$  for later convenience.

<sup>5</sup>Other choices, e.g.,  $\eta(L^-, t) = \alpha\eta(L^+, t) + \beta\partial_x \eta(L^+, t)$ , where  $\alpha$  and  $\beta$  are constants, are conceivable. However, our main conclusion *does not* depend on the boundary condition, because it follows mainly from the linearity of the evolution (32).

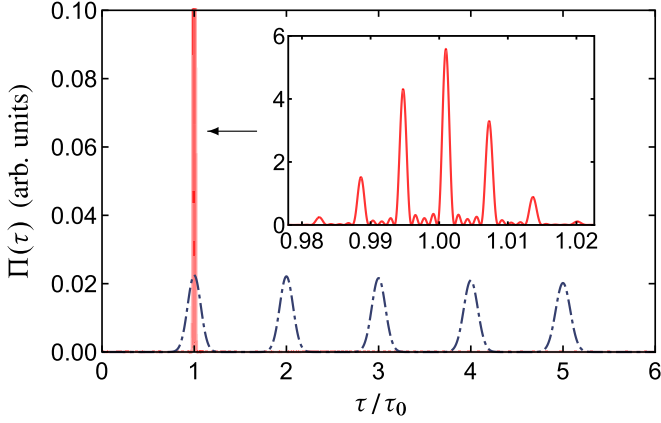


FIG. 2. Illustration of  $\Pi_{\text{SC}}(\tau)$  and  $\Pi_{\text{QF}}(\tau)$  (dot-dashed line) for  $N = 5$ ,  $\sigma = 5$ ,  $L = 10\sigma$ ,  $v = 1$ , and  $\epsilon = 0.05$  (in arbitrary units). The inset shows a magnified view of  $\Pi_{\text{SC}}(\tau)$ .

It follows that

$$\phi(x + kL, k\tau_0) \approx \phi(x, 0)e^{ikvL/2\epsilon}$$

and

$$\begin{aligned} \phi_c(x + kL, t) &\approx e^{-i\delta t H/\hbar} e^{-i(t-k\tau_0-\delta t)\bar{H}/\hbar} \phi(x, 0)e^{ikvL/2\epsilon} \\ &\stackrel{(36)}{=} e^{ikvL/2\epsilon} \phi_c(x, t - k\tau_0). \end{aligned} \quad (40)$$

Hence, by linearity,

$$\psi_c(x, t) \approx \frac{1}{\sqrt{N}} \sum_{k=0}^{N-1} e^{ikvL/2\epsilon} \phi_c(x, t - k\tau_0). \quad (41)$$

Ignoring the tails of the Gaussians, we have that for  $\delta t \ll \tau_0$ , at most only one of the wave packets  $\phi_c(x, t - k\tau_0)$  will have its support in  $(L, L + \Delta)$  at a given time. (Recall that  $\phi_c$  is obtained by free evolution with Dirichlet boundary conditions up until time  $t - \delta t$  and then free evolution for a time  $\delta t$ .) Therefore, we can ignore cross terms of  $|\psi_c(x, t)|^2$  within the interval  $(L, L + \Delta)$  and write

$$\lambda_{\text{JN}}(t) \approx \frac{1}{\delta t} \sum_{k=0}^{N-1} \int_L^{L+\Delta L} dx |\phi_c(x, t - k\tau_0)|^2 \quad (42)$$

so that the property (24) is obtained.

#### IV. SEMICLASSICAL DISTRIBUTION

The semiclassical distribution [cf. Eqs. (3) and (4)] is

$$\Pi_{\text{SC}}(\tau) = \frac{L}{\epsilon\tau^2} \left| \frac{1}{\sqrt{2\pi}} \int_{-\infty}^{\infty} dx \psi(x, 0) e^{-iLx/\epsilon\tau} \right|^2. \quad (43)$$

Using the Fourier transform

$$\begin{aligned} &\frac{1}{\sqrt{2\pi}} \int_{-\infty}^{\infty} dx \phi(x + x_0, 0) e^{-iv_0x/\epsilon} \\ &= \sqrt{\frac{\sigma}{\pi^{1/2}}} \exp\left(\frac{i}{\epsilon} v_0 x_0 - \frac{\sigma^2}{2\epsilon^2} (v - v_0)^2\right), \end{aligned} \quad (44)$$

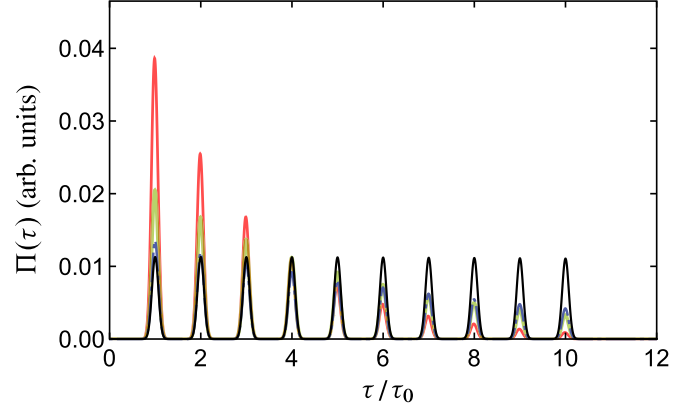


FIG. 3. Illustration of the exponential decay of the arrival-time distributions for a Gaussian wave train satisfying the no spreading condition (20), with the parameters  $N = 10$ ,  $\sigma = 5$ ,  $L = 10\sigma$ ,  $\epsilon = 0.01$ , and  $v = 1$  (in arbitrary units). The red curve is  $\Pi_{\text{JN}}$  with  $\delta t = 0.5$  and  $\Delta L = 0.5\sigma$ , the green curve is  $\Pi_{\text{W}}$  with  $\lambda_0 = 2$ , and the blue curve denotes  $\Pi_{\text{MS}}$  with  $\lambda' = 0.01$ . The black curve is  $\Pi_{\text{QF}}$ , which does not display an exponential decay. The exponential TOF curves were calculated numerically without any approximations (see the text for details).

we find (without approximations) that

$$\begin{aligned} \Pi_{\text{SC}}(\tau) &= \frac{\sigma L}{N\sqrt{\pi}\epsilon\tau^2} \frac{\sin^2(NL^2/2\epsilon\tau)}{\sin^2(L^2/2\epsilon\tau)} \\ &\times \exp\left[-\frac{\sigma^2 v^2}{\epsilon^2} \left(\frac{1 - \tau_0}{\tau}\right)^2\right]. \end{aligned} \quad (45)$$

The distribution is peaked around  $\tau_0$ , contrary to what is anticipated of the Gaussian wave train. This should come as no surprise since  $\Pi_{\text{SC}}$  is fully determined by the momentum distribution of the initial wave function, which in the present example is centered around  $p = mv$ . While the semiclassical distribution sometimes follows from the quantum flux or Bohmian TOF distribution, such is not the case here, as can be seen in Fig. 2. This explains why the latter *does* show the expected behavior, unlike the former.

#### V. DISCUSSION AND OUTLOOK

The exponential distributions for the Gaussian train (18) are plotted in Fig. 3 along with the quantum flux or Bohmian distribution. All arrival-time distributions were produced using the exact analytic expressions without invoking approximations (10) and (20).<sup>6</sup> While the quantum flux distribution displays the expected behavior (i.e., featuring identical and well-separated peaks centered at times  $\tau_0, 2\tau_0, \dots, 10\tau_0$ ) [cf. Eq. (23)], the exponential ones do not, thus substantiating our analysis. The free parameters  $\lambda_0, \lambda', \Delta L$ , and  $\delta t$  were chosen for best visibility. However, this undesirable behavior cannot

<sup>6</sup>For the Jurman-Nikolić proposal, we used  $\lambda_{\text{JN}}(t) \approx (\Delta L/\delta t)|\psi_c(L, t)|^2$ , applicable for a small  $\Delta L$ . However,  $\psi_c(x, t)$  of Eq. (35) was evaluated exactly in terms of error functions by integrating (27) against the known free-particle propagator for time  $\delta t$ .

be evaded by tuning these parameters: Making them larger causes a faster decay, while making them smaller moderates the decay at the cost of increasing the nondetection probability (to the extent of a vanishing arrival-time density in the case of an appreciable removal of the decay). In fact, given any choice of these free parameters, the number  $N$  of Gaussians in the train and their velocity  $v$  could be so chosen that the exponential decay practically washes out the arrival-time peaks corresponding to the trailing Gaussians.

The exponential proposals were aimed at deriving the TOF distribution by means of a detector model. While different intensity functions  $\lambda$  can be considered, our results show that the failure is not so much attributable to the particular choice of  $\lambda$  but presumably the assumption of independence that underlies the Poisson process.

While it is, as a matter of principle, necessary to account for the effect of the detector in *any* experiment, the extent to which the physics of the detector needs to be taken seriously for predicting arrival times is not self-evident. In practice, scattering experiments such as the double-slit and the Stern-Gerlach experiment are routinely analyzed with no reference whatsoever to the detector. However, since the detectors employed in these experiments are typically no more specialized than the ones found in TOF experiments (e.g., a scintillation screen employed in [1]), it is not *a priori* obvious why the physics of the detector is any more relevant for predicting the statistics of arrival times than it is for predicting the statistics of impact positions. Hence it should not come as a surprise

that the quantum flux distribution gives the anticipated result despite ignoring the detector. It has even been shown that  $\Pi_{\text{QF}}(\tau)$  can arise from a careful consideration of a physical detector, e.g., a laser curtain inducing fluorescence from an incoming atom [40–42]. This suggests that one should turn to realistic TOF experiments if one wants to take the detector seriously.

Finally, the semiclassical distribution depicted in Fig. 2 also fails to display the intended behavior since it is largely supported around  $\tau_0$ . This distribution is often used in the experimental determination of the momentum distribution. Using the measured arrival-time distribution  $\Pi_{\text{meas}}(\tau)$ , the empirical momentum distribution is taken to be

$$\frac{mL}{p^2} \Pi_{\text{meas}}\left(\frac{mL}{p}\right), \quad (46)$$

corresponding to the quantum mechanical momentum distribution  $\hbar^{-1} |\tilde{\psi}(p/\hbar)|^2$ , thereby tacitly assuming the validity of (3). However, our results indicate that such reconstructions are questionable (see also [26], Chap. 4).

#### ACKNOWLEDGMENTS

W.S. was supported by the Research Foundation Flanders (Fonds Wetenschappelijk Onderzoek), Grant No. G066918N. It is a pleasure to thank J. M. Wilke for valuable editorial input.

- 
- [1] C. Kurtsiefer, T. Pfau, and J. Mlynek, *Nature (London)* **386**, 150 (1997); T. Pfau and C. Kurtsiefer, *J. Mod. Opt.* **44**, 2551 (1997); C. Kurtsiefer and J. Mlynek, *Appl. Phys. B* **64**, 85 (1996).
- [2] J. Ullrich, R. Moshhammer, A. Dorn, R. Dörner, L. P. H. Schmidt, and H. Schmidt-Böcking, *Rep. Prog. Phys.* **66**, 1463 (2003).
- [3] A. Kothe, J. Metje, M. Wilke, A. Moguevski, N. Engel, R. Al-Obaidi, C. Richter, R. Golnak, I. Y. Kiyani, and E. F. Aziza, *Rev. Sci. Instrum* **84**, 023106 (2013).
- [4] A. Gliserin, M. Walbran, and P. Baum, *Rev. Sci. Instrum* **87**, 033302 (2016).
- [5] S. Wolf and H. Helm, *Phys. Rev. A* **62**, 043408 (2000).
- [6] L. Schnieder, K. Seekamp-Rahn, E. Wrede, and K. H. Welge, *J. Chem. Phys.* **107**, 6175 (1997).
- [7] Y. Xie, H. Zhao, Y. Wang, Y. Huang, T. Wang, X. Xu, C. Xiao, Z. Sun, D. H. Zhang, and X. Yang, *Science* **368**, 767 (2020).
- [8] A. Fuhrmanek, A. M. Lance, C. Tuchendler, P. Grangier, Y. R. P. Sortais, and A. Browaeys, *New J. Phys.* **12**, 053028 (2010).
- [9] F. Stopp, L. G. Ortiz-Gutiérrez, H. Lehec, and F. Schmidt-Kaler, *New J. Phys.* **23**, 063002 (2021).
- [10] J. G. Muga and C. R. Leavens, *Phys. Rep.* **338**, 353 (2000).
- [11] J. Muga, R. Sala, and J. Palao, *Superlatt. Microstruct.* **23**, 833 (1998).
- [12] *Time in Quantum Mechanics*, 2nd ed., edited by J. G. Muga, R. S. Mayato, and Í. L. Egusquiza, Lecture Notes in Physics Vol. 734 (Springer, Berlin, 2008).
- [13] M. Daumer, D. Dürr, S. Goldstein, and N. Zanghi, *J. Stat. Phys.* **88**, 967 (1997); M. Daumer, D. Dürr, S. Goldstein, and N. Zanghi, *Lett. Math. Phys.* **38**, 103 (1996).
- [14] C. R. Leavens, *Phys. Rev. A* **58**, 840 (1998); *Superlatt. Microstruct.* **23**, 795 (1998).
- [15] G. Grübl and K. Rheinberger, *J. Phys. A: Math. Gen.* **35**, 2907 (2002); S. Kreidl, G. Grübl, and H. G. Embacher, *ibid.* **36**, 8851 (2003).
- [16] S. Das and M. Nöth, *Proc. R. Soc. A* **477**, 20210101 (2021).
- [17] A. J. Bracken and G. F. Melloy, *J. Phys. A: Math. Gen.* **27**, 2197 (1994).
- [18] M. V. Berry, *J. Phys. A: Math. Theor.* **43**, 415302 (2010).
- [19] M. Penz, G. Grübl, S. Kreidl, and P. Wagner, *J. Phys. A: Math. Gen.* **39**, 423 (2005).
- [20] J. M. Yearsley and J. J. Halliwell, *J. Phys.: Conf. Ser.* **442**, 012055 (2013).
- [21] A. Goussev, *Phys. Rev. A* **99**, 043626 (2019).
- [22] I. L. Egusquiza and J. G. Muga, *Phys. Rev. A* **61**, 012104 (1999).
- [23] J. Kijowski, *Rep. Math. Phys.* **6**, 361 (1974).
- [24] C. Kurtsiefer, T. Pfau, C. R. Ekstrom, and J. Mlynek, *Appl. Phys. B* **60**, 229 (1995).
- [25] J. R. Copley and T. J. Udovic, *J. Res. Natl. Inst. Stand. Technol.* **98**, 71 (1993).
- [26] N. Vona, [arXiv:1403.2496](https://arxiv.org/abs/1403.2496) [math-ph].

- [27] R. Werner, *Ann. Phys. Theor.* **47**, 429 (1987).
- [28] R. Tumulka, [arXiv:1601.03715](https://arxiv.org/abs/1601.03715).
- [29] J. J. Halliwell and J. M. Yearsley, *Phys. Rev. A* **79**, 062101 (2009).
- [30] J. G. Muga, J. P. Palao, and C. R. Leavens, *Phys. Lett. A* **253**, 21 (1999).
- [31] G. R. Allcock, *Ann. Phys. (NY)* **53**, 286 (1969).
- [32] J. Echanobe, A. del Campo, and J. G. Muga, *Phys. Rev. A* **77**, 032112 (2008).
- [33] D. Jurman and H. Nikolić, *Phys. Lett. A* **396**, 127247 (2021).
- [34] P. Blanchard and A. Jadczyk, *Helv. Phys. Acta* **69**, 613 (1996).
- [35] P. Blanchard and A. Jadczyk, *Int. J. Theor. Phys.* **37**, 227 (1998).
- [36] A. Marchewka and Z. Schuss, *Phys. Lett. A* **240**, 177 (1998); *Phys. Rev. A* **63**, 032108 (2001); **65**, 042112 (2002).
- [37] L. Maccone and K. Sacha, *Phys. Rev. Lett.* **124**, 110402 (2020).
- [38] S. Das and D. Dürr, Benchmarking quantum arrival-time distributions using a back-wall (unpublished).
- [39] J. J. Włodarz, *Phys. Rev. A* **65**, 044103 (2002).
- [40] J. A. Damborenea, Í. L. Egusquiza, G. C. Hegerfeldt, and J. G. Muga, *Phys. Rev. A* **66**, 052104 (2002).
- [41] J. A. Damborenea, Í. L. Egusquiza, G. C. Hegerfeldt, and J. G. Muga, *J. Phys. B* **36**, 2657 (2003).
- [42] V. Hannstein, G. C. Hegerfeldt, and J. G. Muga, *J. Phys. B* **38**, 409 (2005).